Vol. 5(17) Oct. 2015, PP. 2375-2397

Contents list available at IJMEC

International Journal of Mechatronics, Electrical and Computer Technology (IJMEC)

Journal Homepage: www.aeuso.org

PISSN: 2411-6173 - EISSN: 2305-0543

Utilization of Terminal Sliding mode in Finite Time Control of Underwater Slave and Land based Master Robotic Manipulators

Fariba Rahimi[1*], Majid Siami[2] and Mohamed Madadpour Inallou[3]

Mechatronics Engineering, KTH Royal Institute of Technology, Stockholm, Sweden

Mechanical Engineering, University of Tabriz, Tabriz, Iran

Young Researchers and Elite Club, West Tehran Branch, Islamic Azad University, Tehran, Iran

***Corresponding Author's E-mail:** fariiba.rahimi@gmail.com*

Abstract

This paper proposed a robust control method for a land-based master and an underwater slave robotic manipulator. In order to comprehend the synchronization between the two diverse systems with the existing uncertainties, external disturbances and fully unknown parameters are considered. For a robust position tracking control of the underwater slave manipulator, an adaptive terminal sliding mode control method has been suggested. It is capable of attaining stability for master and slave manipulators operating in unknown environments with time-varying uncertainties such as added mass, buoyancy, hydraulic drag and friction effect. An improved robust adaptive continuous finite-time control scheme with a form of terminal sliding mode achieved by the boundary layer approach for land (master) and underwater (slave) manipulators is highly effective in reducing the abovementioned problems. In Under water conditions, robot is simulated and torques exerted from water on the links were be calculated. The proposed method is presented and its effectiveness is demonstrated through simulation and experimental results. These results verify the faster tracking performance of the proposed method and its accuracy and robustness in the presence of uncertainties and hydrodynamic and exogenous disturbances. The experimental results confirm the superior performance of the proposed control method.

Keywords: *underwater manipulator slave system, land-based master system, terminal sliding mode, synchronization.*

1. Introduction

Underwater robotic manipulators play a significant role in shallow or deep water operations related to maritime science, oil and gas exploration and inspection and military applications [1,2] These manipulators are usually operated in a master-slave scheme by an operator on a surface vessel [3]. The special theorems and the challenging issues that exist for the control of underwater manipulators make the control of such devices difficult. These include the high degree of nonlinearity and the time-varying dynamic behavior of the vehicle, uncertainties in the hydrodynamic coefficients, the higher order and the redundancy when a manipulator is attached, disturbances by ocean currents and the changes in the centers of gravity and buoyancy due to the motion of the manipulator, which disrupts the vehicle [4]. To overcome these problems in the control of underwater manipulators, a robust adaptive terminal-sliding mode-control model for the dynamic positioning and trajectory tracking of master and slave manipulators is suggested. Calculated torque control leads to the asymptotic stability of robot manipulators [5]. The asymptotic stability that results by the SMC method infers that the system trajectories converge to equilibrium. Nevertheless,

Article History:

Received Date: Jun. 24, 2015

Accepted Date: Sep. 09, 2015

Available Online: Sep. 10, 2015

the finite-time stabilization of the dynamic systems may give rise to a high-precision performance in addition to finite-time convergence to equilibrium. It is obtained in [6,7]. This approach has been used to control the robotic manipulators [8]. Nonetheless, the robustness issue has not been fully addressed. So far, for controlling underwater manipulators, numerous control methods have been suggested including the sliding-mode control, which is easy to apply and has robust [9]. The researchers in [10]. Have applied this method quite successfully and used a series of single-input single-output (SISO) continuous time controllers. They have ultimately examined the effects of uncertainties on hydrodynamic coefficients and ignored the cross-coupling terms. In [11], to control an underwater vehicle in the dive plane, an adaptive sliding mode controller was proposed and a control law based on a linear model with no information on the nonlinear characteristics of vehicle dynamics was extended. In [12] to control a ROV (Remotely Operated Vehicle), a sliding mode control was used that disregarded the Coriolis and centrifugal terms in the dynamic model of the ROV. However, all these mentioned studies needed to have the boundaries for uncertainties in advance. In this study, however, we have challenged the problem of acquiring the boundaries for uncertainties. Among all the previous works, no study has fully considered the dynamics of the problem when dealing with the synchronization of land-based master and underwater slave manipulators. Additionally, robust adaptive terminal sliding mode control has not yet been applied within a finite time for land-based master and underwater slave manipulators.

In this paper, an improved continuous terminal sliding mode controller has been used for a master-slave underwater manipulator system, which provides finite-time stabilization as well as high-precision performance in addition to finite-time convergence to equilibrium. By applying this controller, finite time convergence is achieved. The use of the boundary layer approach leads to the highest efficiency in the reduction of control chatter. However, the TSM controller is slightly more complex in comparison with the conventional sliding mode control. For the trajectory tracking of the master and slave systems, synchronization has been implemented between these two different systems. Eventually a slave system is obtained with a great position and velocity tracking ability of the master system and a continuous and chatter-free control. This fact is demonstrated through the simulation results pertaining to the application of a robust adaptive terminal sliding mode control. It should be noted that the improved continuous terminal sliding mode controller with adaptive control has not yet been used for synchronizing a surface master manipulator and an underwater slave manipulator. Furthermore, in this study, the dynamics of master and slave manipulators has been thoroughly considered and discussed.

The rest of this paper is organized as follows. In Section 2, the dynamic manipulator models for a 2-DOF land based manipulator (as the master system) and an underwater manipulator (as the slave system) and also the extra forces involved in the dynamics of an underwater robotic system are presented. Section 3 explains the continuous terminal sliding mode controller. The synchronization between master and slave systems is covered in Section 4. In Section 5, the theoretical and experimental simulations are performed to establish the capability and effectiveness of the proposed controller. The study is concluded in Section 6.

2. Dynamic manipulator model

In this section, the difference between the dynamics of an underwater manipulator and a land-based manipulator is investigated by considering the hydrodynamic and hydrostatic effects in the dynamic function of the underwater manipulator. A 2-DOF manipulator configuration is dynamically modeled [13].

The general dynamic model of an n-axis land-based manipulator (master) is shown in Eq. 1,

$$M_m(q_m)\ddot{q}_m + C_m(q_m, \dot{q}_m)\dot{q}_m + G_m(q_m) = \tau_m \quad (1)$$

Where index 'm' denotes master system, q_m is the $n\times1$ joint angle vector of the master manipulator, $M_m(q_m)$ is the $n\times n$ inertia matrix, $C_m(q_m,\dot{q}_m)$ is the $n\times n$ Coriolis and centripetal matrix, $G_m(q_m)$ is the gravity factor, and τ_m represents the input torque of the master manipulator [14].

2.1. Underwater manipulator (slave)

Considering the hydrodynamic, hydrostatic and other forces that exist in an underwater environment, the dynamics of an underwater manipulator will be different from that of a surface manipulator. If a robot is operated underwater, additional forces and moments are exerted on it due to the impressive mass of the fluid surrounding the robot that must be accelerated as the robot moves. The equation of motion for an underwater manipulator (slave) which has n-joints is as follows [13]:

$$M_s(q_s)\ddot{q}_s+C_s(q_s,\dot{q}_s)\dot{q}_s+D_s(\dot{q}_s)+F_s^*(\dot{q}_s)+h_s(q_s)=\tau_s \quad (2)$$

In this equation, index 's' denotes the slave manipulator, q_s is the angular position of the slave manipulator joint, $M_s(q_s)$ is the inertia matrix, $C_s(q_s,\dot{q}_s)$ indicates the Coriolis and centrifugal forces, $h_s(q_s)$ denotes the gravity forces which comprise the buoyancy effects, $F_s^*(\dot{q}_s)$ is the friction force, $D_s(\dot{q}_s)$ is the hydraulic drag force which is affected by the velocity of manipulator relative to ocean current and waves, and τ_s is the vector of applied joint torques which actually constitute the control inputs. To precisely model the underwater manipulator in this study, four major hydrodynamic properties (i.e., added mass, added Coriolis and centripetal forces, drag force and buoyancy force) have been considered [13].

2.1.1 Hydrodynamics

2.1.1.1 Added mass: When a rigid body moves in a fluid, added mass is produced. The fluid is accelerated by the movement of the body, which requires an additional force. Due to the low density of air relative to water, which almost has the same density as the underwater vehicle, this influence is neglected in typical industrial robotic applications [15].

$M(q)$ and $C(q,\dot{q})$ for an underwater slave manipulator vary from those for a surface master manipulator, because they include added mass [13]. The matrices of the dynamic equation for a 2-DOF underwater planar manipulator are shown in the Appendix.

2.1.1.2 Drag force: The drag force applied on the links of the manipulator is modeled based on the Strip Theory. The strip theory is applied by substituting the surface integral by a line integral along the length of the links. Different drag coefficients have been presented by [15]). The drag coefficient is obtained by Eq. 3 [16].

$$\tau=-\sum_{i=1}^{n}C_d\left(\frac{l_i\theta}{D}\right)*0.5\rho Dl_i^3dl_i\left|\dot{\theta}\right|\dot{\theta} \quad (3)$$

In this equation, C_d is the drag coefficient, D is the diameter of the cylinder, θ is the joint displacement and l shows the distance from the joints to the segmented length [13].

2.1.2. Hydrostatics

2.1.2.1. Buoyancy: In the static analysis of underwater bodies, both the gravitational and buoyancy forces acting on a submerged body must be considered. The volume of fluid displaced by the submerged body creates an upward a force called buoyancy. This force acts at the body's center of buoyancy (i.e., the center of fluid volume displaced by the body [17] in a direction

opposite to the gravitational force. The gravity force acting on the submerged body mass is determined as [13]:

$$F_{buoyancy} = \rho V g \quad (4)$$

$$F_{gravity} = mg \quad (5)$$

$$(h = F_{buoyancy} - F_{gravity}) \quad (6)$$

where g is the vector of acceleration due to gravity acting at the center of mass, V is the volume displaced by the body, ∇ or ρV is the mass of water displaced by the link, and m is the link mass [13]. The matrix of the dynamic equation for a 2-DOF underwater manipulator is shown in the Appendix.

2.1.3. Friction force

F^* denotes the friction force, which is eventuated as Eq. 7 [13].

$$F^* = F_v + F_c \quad (7)$$

$$F_v = \begin{bmatrix} k_{v1}\dot{q}_1 \\ k_{v2}\dot{q}_2 \end{bmatrix} \quad (8)$$

$$F_c = \begin{bmatrix} k_{c1} sign(\dot{q}_1) \\ k_{c2} sign(\dot{q}_2) \end{bmatrix} \quad (9)$$

In this equation, F_v and F_c denote the viscous and coulomb friction torques, respectively. The hydrodynamic coefficient (C_d) for link1 and link2 are taken to be 0.1624 and .078 respectively, and the water density (ρ) is selected as $1025\ kg/m^3$. The friction coefficients are as follows: $k_{v2} = k_{c2} = 0.5, k_{v1} = 0.3, k_{c1} = 0.2$.

3. Terminal sliding mode (TSM)

In this paper, a form of TSM and some of their features, as introduced in [14], are considered for synchronizing the control of master and slave manipulators. The results demonstrate that the proposed method has a fast and precise tracking capability and is accurate and robust with respect to hydrodynamic disturbances.

3.1. Structure of robust adaptive continuous finite-time control for master-slave manipulators

As in this heading, they should be Times New Roman 11-point boldface, initially capitalized, flush left, with one blank line before, and one after.

For the trajectory tracking of master and slave manipulators, an improved continuous finite-time control with a form of TSM introduced in [14] has been established. In this control scheme, because of a faster convergence speed compared with conventional continuous sliding-mode control methods, a more precise tracking is achieved.

As shown in Eqs. (1) and (2), the dynamics of n-link master and slave robotic manipulators, used in designing an adaptive controller, is written as Eqs. (10-a) & (10-b), respectively.

$$M_m(q_m)\ddot{q}_m + C_m(q_m, \dot{q}_m)\dot{q}_m + G_m(q_m) + \delta_m = \tau_m \quad (10\text{-a})$$

$$M_s(q_s)\ddot{q}_s + C_s(q_s, \dot{q}_s)\dot{q}_s + D_s(\dot{q}_s) + F_s^*(\dot{q}_s) + h_s(q_s) + \delta_s = \tau_s \quad (10\text{-b})$$

with

$$\delta_m = \Delta M_m(q_m)\ddot{q}_m + \Delta C_m(q_m, \dot{q}_m)\dot{q}_m + \Delta G_m(q_m) \quad (11\text{-a})$$

$$\delta_s = \Delta M_s(q_s)\ddot{q}_s + \Delta C_s(q_s,\dot{q}_s)\dot{q}_s + \Delta D_s(\dot{q}_s) + \Delta F^*_s(\dot{q}_s) + \Delta h_s(q_s) \quad (11\text{-b})$$

In these equations, δ_m and δ_s denote the perturbation that includes all the uncertainty terms and environmental disturbances in the system [8] and $\tau_{d_m}, \tau_{d_s} \in R^n$ with $\|\tau_{d_m}\| \le d$ and $\|\tau_{d_s}\| \le d$ are the vectors of the restricted external disturbances. So, the dynamic models of the master and slave manipulators are revised as [14]:

$$M_m(q_m)\ddot{q}_m + C_m(q_m,\dot{q}_m)\dot{q}_m + G_m(q_m) = \tau_m + \tau_{d_m} + L_{d_m}(q_m,\dot{q}_m,\ddot{q}_m) \quad (12\text{-a})$$

$$M_s(q_s)\ddot{q}_s + C_s(q_s,\dot{q}_s)\dot{q}_s + D_s(\dot{q}_s) + F^*_s(\dot{q}_s) + h_s(q_s) = \tau_s + \tau_{d_s} + L_{d_s}(q_s,\dot{q}_s,\ddot{q}_s) \quad (12\text{-b})$$

Where $L_{d_m}(q_m,\dot{q}_m,\ddot{q}_m)$ and $L_{d_s}(q_s,\dot{q}_s,\ddot{q}_s)$ are the lumped system uncertainties. By comparing Eqs. (10-a) and (10-b) with Eqs. (11-a) and (11-b), the following equations are obtained:

$$L_{d_m}(q_m,\dot{q}_m,\ddot{q}_m) + \tau_{d_m} = -\Delta M_m(q_m)\ddot{q}_m - \Delta C_m(q_m,\dot{q}_m)\dot{q}_m - \Delta G_m(q_m) \in R^n \quad (13\text{-a})$$

$$L_{d_s}(q_s,\dot{q}_s,\ddot{q}_s) + \tau_{d_s} = -\Delta M_s(q_s)\ddot{q}_s - \Delta C_s(q_s,\dot{q}_s)\dot{q}_s - \Delta D_s(\dot{q}_s) - \Delta F_s^*(\dot{q}_s) - \Delta h_s(q_s) \in R^n \quad (13\text{-b})$$

These equations are assumed to be restricted by the following functions [17]:

$$\|L_{d_m}(q_m,\dot{q}_m,\ddot{q}_m)\| + \|\tau_{d_m}\| \le b_0 + b_1\|q_m\| + b_2\|\dot{q}_m\|^2 \quad (14\text{-a})$$

$$\|L_{d_s}(q_s,\dot{q}_s,\ddot{q}_s)\| + \|\tau_{d_s}\| \le b_3 + b_4\|q_s\| + b_5\|\dot{q}_s\|^2 \quad (14\text{-b})$$

To design the terminal sliding mode controller for a master-slave underwater manipulator, an improved type of terminal sliding surface has been defined below:

$$s = \tilde{q} + \alpha\int \tilde{q} + \beta|\dot{\tilde{q}}|^{\gamma}\, sign(\dot{\tilde{q}}) = 0 \quad (15)$$

So for slave and master manipulators the sliding surface will be defined as below equations respectively:

$$s_s = \tilde{q}_s + \alpha\int \tilde{q}_s + \beta|\dot{\tilde{q}}_s|^{\gamma}\, sign(\dot{\tilde{q}}_s) = 0 \quad (15\text{-1})$$

$$s_m = \tilde{q}_m + \alpha\int \tilde{q}_m + \beta|\dot{\tilde{q}}_m|^{\gamma}\, sign(\dot{\tilde{q}}_m) = 0 \quad (15\text{-2})$$

where $s_m, s_s = [s_1,...,s_n]^T \in R^n$, $\beta = diag(\beta_1,...,\beta_n)$ and $1 < \gamma_i,...,\gamma_n < 2$. This sliding surface will actually force the error vector to approach zero [14].

$$sig(x)^{\gamma} = \left[|x_1|^{\gamma_1} sign(x_1),...,|x_n|^{\gamma_n} sign(x_n)\right]^T,$$

$$x^{\gamma} = \left[x_1^{\gamma_1},...,x_n^{\gamma_n}\right],\quad |x|^{\gamma} = \left[|x_1|^{\gamma_1},...,|x_n|^{\gamma_n}\right]. \quad (16)$$

The smaller value of β in Eq. (18) accelerates the convergence rate.The tracking error vector of master ($\tilde{q}_m$) is defined as

$$\tilde{q}_m = q_m - q_{d\_m}, \quad (17)$$

Suppose that the human operator as a desired input trajectory for the master manipulator as represented by q_{d_m}, which was chosen to be sinusoidal in this study. The aim of the control scheme is to find feedback controls $\tau_m(q,\dot{q})$ and $\tau_s(q,\dot{q})$ such that the slave manipulator output q_s follows the master manipulator trajectory and the master manipulator q_m tracks the desired reference trajectory q_{d_m} in finite time [14].

Considering a Lyapunov function similar to the one expressed in [13], control forces τ_s and τ_m are chosen as Eqs. (18-a) and (18-b), respectively.

$$\tau_s = \tau_{cont\_s} + \tau_{dis\_s} \quad (18\text{-a})$$

$$\tau_m = \tau_{cont\_m} + \tau_{dis\_m} \quad (18\text{-b})$$

With

$$\tau_{cont\_s} = M_s(q_s)\left(\ddot{q}_{d\_s} + \dot{q}_{d\_s} - \dot{q}_s\right) + C_s(q_s,\dot{q}_s)\dot{q} + D_s(\dot{q}_s) + F_s^*(\dot{q}_s) + h_s(q_s) - M_s(q_s)\beta^{-1}\gamma^{-1}sig(\dot{\tilde{q}}_s)^{2-\gamma} \quad (19\text{-a})$$

$$\tau_{cont\_m} = M(q_m)\left(\ddot{q}_{d\_m} + \dot{q}_{d\_m} - \dot{q}_m\right) + C_m(q_m,\dot{q}_m)\dot{q} + G_m(q_m) - M_m(q_m)\beta^{-1}\gamma^{-1}sig(\dot{\tilde{q}}_m)^{2-\gamma} \quad (19\text{-b})$$

and

$$\tau_{dis\_s} = -M_s(q_s)(k_1 s + k_2 sig(s_s)^{\rho}), \quad (20\text{-a})$$

$$\tau_{dis\_m} = -M_m(q_m)(k_1 s + k_2 sig(s_m)^{\rho}) \quad (20\text{-b})$$

Where $\gamma = diag(\gamma_1,...,\gamma_n)$ and $k_1 = diag(k_{11},...,k_{1n})$, $k_2 = diag(k_{21},...,k_{2n})$, $k_{1i}, k_{2i} > 0$, $0 < \rho = \rho_1 = ... = \rho_n < 1$.

The control laws in Eqs. (18-a) and (18-b) are continuous and, consequently, chatter-free. They do not include any negative fractional powers; hence, they are also singularity-free. By selecting $0 < 2-\gamma_i < 1$ and $0 < \rho < 1$, the control scheme becomes robust and chatter-free [14].

To make the control discontinuity caused by $sign(s)$ smooth, a boundary layer is used in control laws (23-a) and (23-b) to eradicate the control chatter [18].

$$\dot{s} = -k_1 s - k_2 sign(s), \quad sign(s) = \begin{cases} \dfrac{s}{\|s\|}, & \|s\| \neq 0, \\ 0, & \|s\| = 0, \end{cases} \quad (21)$$

$$\dot{s} = -k_1 s - k_2 sat(\frac{s}{\varepsilon}), \quad sat(\frac{s}{\varepsilon}) = \begin{cases} \dfrac{s}{\|s\|}, & \|s\| \geq \varepsilon, \\ \dfrac{s}{\varepsilon}, & \|s\| < \varepsilon, \end{cases} \quad (22)$$

In these relations, ε denotes the width of the boundary layer. Because of the discontinuity in the control law, exhaustive chattering will appear in practice. Boundary layer $\|s_m, s_s\| < \varepsilon$ is achieved by continuous control τ_m and τ_s [14], where:

$$\tau_{dis\_m} = -(k_1 s_m + k_2 sat(\frac{s_m}{\varepsilon})^{\rho}), \quad k_1, k_2 > 0 \quad (23\text{-a})$$

$$\tau_{dis\_s} = -(k_1 s_s + k_2 sat(\frac{s_s}{\varepsilon})^{\rho}), \quad k_1, k_2 > 0 \quad (23\text{-b})$$

For controls (18-a) and (18-b), a small value of ε is chosen, and k_1 and k_2 are chosen through trial and error.

4. Synchronization

Ideal synchronization will be achieved for the proposed controller if the output of the slave system follows the output of the master system which tracks the desired input in finite time. Hence, the main purpose of this study is to design a robust adaptive terminal sliding mode controller (RATSMC) to synchronize two different systems (master and slave manipulators) with totally unknown parameters, in the presence of uncertainties and external disturbances. It is presumed that the bounds of the uncertainties and external disturbances are not known in advance. An appropriate terminal sliding surface, which contains synchronization errors, is constructed. Consequently, to tackle the uncertainties, external disturbances and unknown parameters, suitable update laws are applied. To solve the synchronization problem, the error between the master and slave systems is expressed as $\ddot{\tilde{q}}_s(t) = \ddot{q}_s - \ddot{q}_m$, where q_m is the desired position (q_{d_s}) for the slave manipulator. Then we have

$$\ddot{q}_s = M_s^{-1}(q_s)[\tau_s + L_{d_s}(q_s, \dot{q}_s, \ddot{q}_s) - C_s(q_s, \dot{q}_s)\dot{q}_s - D_s(\dot{q}_s) - F_s^*(\dot{q}_s) - h_s(q_s) - \delta_s] \quad \text{(24-a)}$$

$$\ddot{q}_m = M^{-1}(q_m)[\tau_m + L_{d_m}(q_m, \dot{q}_m, \ddot{q}_m) - C(q_m, \dot{q}_m)\dot{q}_m - G(q_m) - \delta_m] \quad \text{(24-b)}$$

Now, by subtracting Eq. (24-b) from Eq. (24-a), the error of the slave system is obtained as [19]:

$$\ddot{\tilde{q}}_s = M^{-1}(q_s)[\tau_s + F(q_s, \dot{q}_s, \ddot{q}_s) - C(q_s, \dot{q}_s)\dot{q}_s - D(\dot{q}_s) - F(\dot{q}_s) - h(q_s) - \delta_s] - M^{-1}(q_m)[\tau_m + F(q_m, \dot{q}_m, \ddot{q}_m) - C(q_m, \dot{q}_m)\dot{q}_m - G(q_m) - \delta_m] \quad \text{(25)}$$

$$\tilde{q}_s = \frac{1}{s^2}\ddot{\tilde{q}}_s \quad \text{(26)}$$

The synchronization problem is converted to a corresponding problem of stabilizing the system error. For a land-based master system and an underwater slave system with uncertainties, external disturbances and unidentified parameters, this paper attempts to design appropriate feedback control laws τ_m and τ_s so that the resulting error system is stabilized, in the sense that $x(t) \to y(t)$; i.e., $q_m \to q_{m\_s}$ and $q_s \to q_{d\_s}$ in finite time [19].

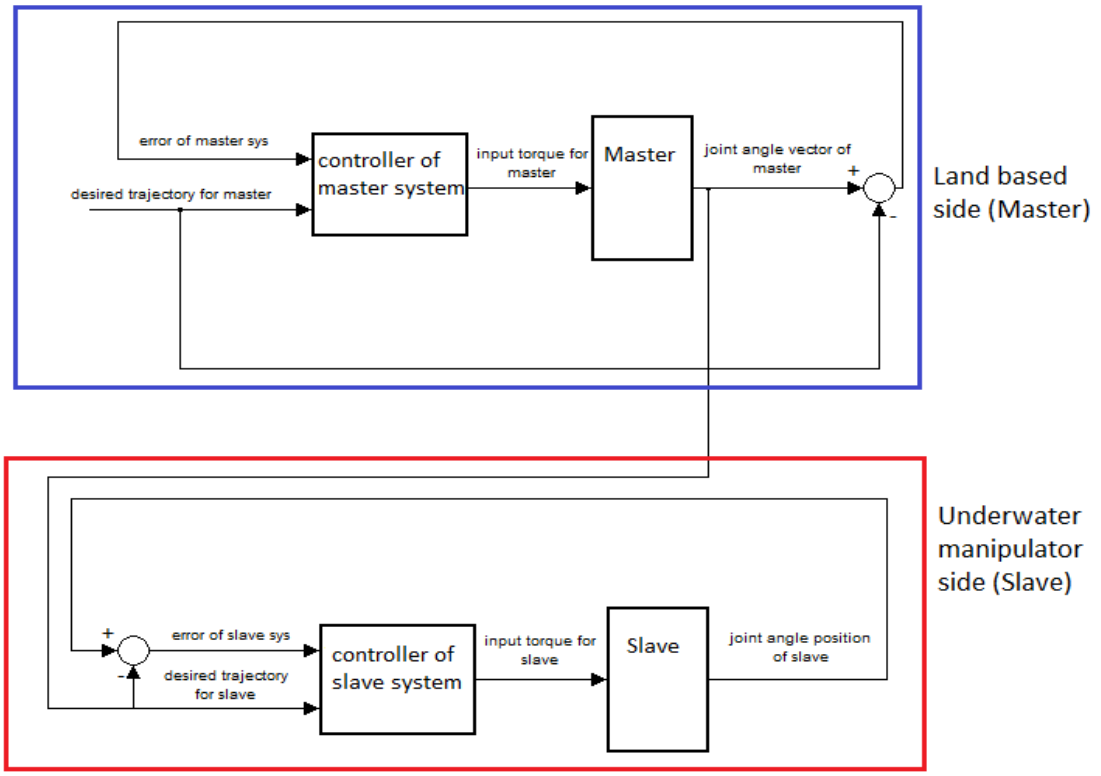

Figure 1: Synchronization of two different uncertain systems using a robust terminal sliding mode controller

5. Theoretical simulation

Considering the simulation example of a 2-link underwater manipulator in [13], for an underwater master-slave system with its dynamic equations given in the appendix we have:

Table 1 gives the parameters of both links. l_i, r_i and m_i are the length, radius and mass of link i, respectively.

Table 1: Parameters of links in theoretical analysis [17]

Link 1 and 2 parameters	Value
l_1	0.543 m
l_2	0.337 m
r_1	0.075 m
r_2	0.075 m
m_1	30.0 kg
m_2	20.0 kg
m_{a1}	39.84 kg
m_{a2}	26.1 kg
k_{c2}, k_{v2}	0.5
k_{c1}	0.2
k_{v1}	0.3
ρ	$1025\ kg/m^3$
c_d	1.1
g	9.81 m/s^2

The bounds of system uncertainties in (17-a) and (17-b) are assumed to be $b_0 = 1.5, b_1 = 1.2, b_2 = 1.8$. For the nominal system, the control parameters are chosen as $k_1 = 50, k_2 = 40, \rho = 0.1, \eta = 1.9, \beta = 200$.

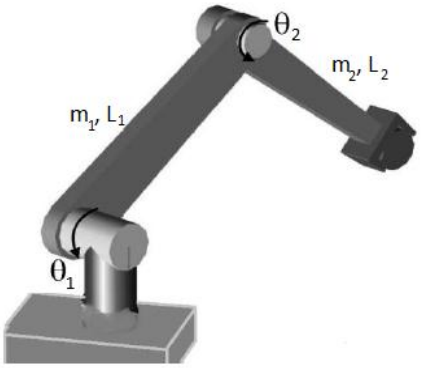

Figure 2: Two- DOF manipulator

The simulation results related to the synchronization of the two different systems (master and slave manipulators) with two links shown in Fig. 2, which have been obtained by the proposed robust adaptive terminal sliding mode control law in (18-a) and (18-b), are presented below:

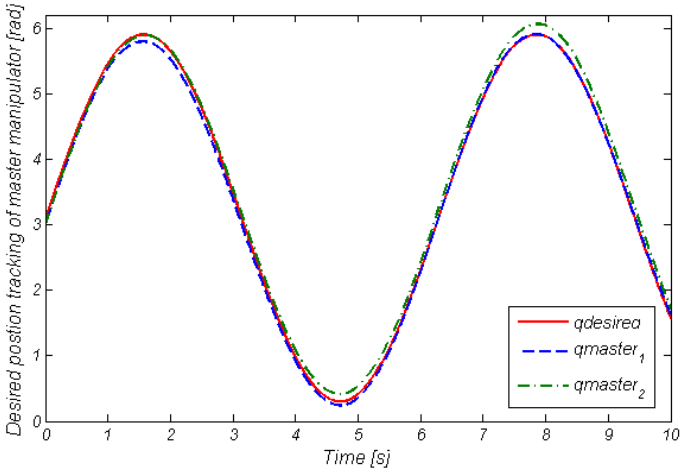

Figure 3: Desired position trajectory and tracking of it by two-links of master manipulator

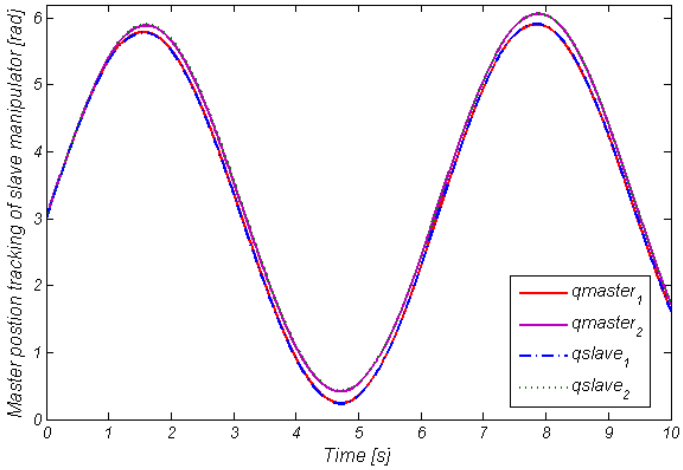

Figure 4: Position tracking signals of two-link master manipulator by two-link slave manipulators

From Fig. 3 and Fig. 4, it is apparent that link 1 and link 2 positions of the slave manipulator accurately follow link 1 and link 2 positions of the master manipulator, respectively, in finite time, which precisely follow the desired sinusoidal positions in finite time, and consequently cause the signal error to be very small. The maximum position and velocity tracking errors of the proposed control scheme are renunciation values (as shown in Fig. 5).

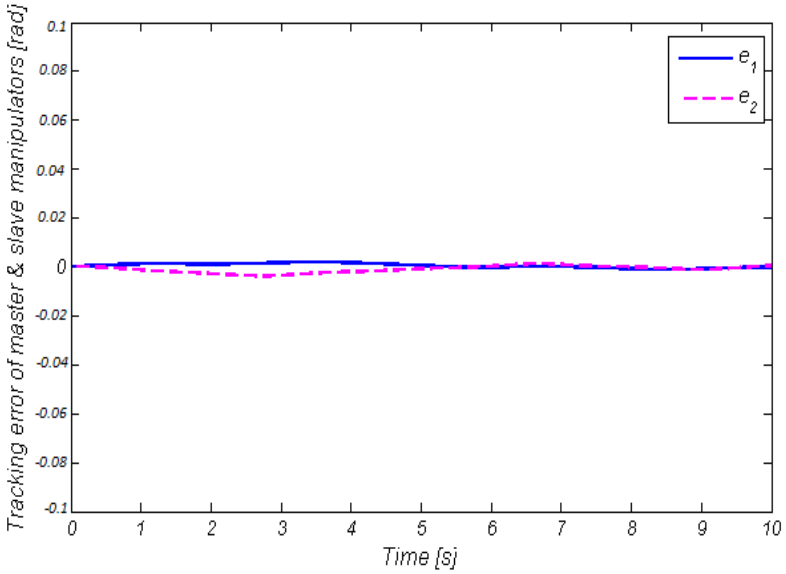

a) Position

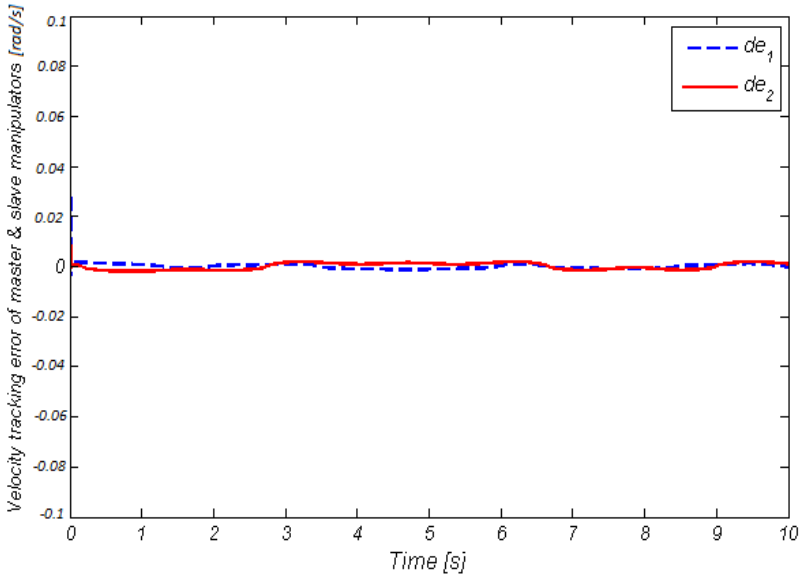

b) Velocity

Figure 5: Tracking errors

The sliding surfaces for the finite time convergence of master and slave systems are shown in Fig. 6. According to this figure, after a few seconds, the sliding surfaces lead to the best position and velocity tracking performance in finite time with negligible error, and ultimately ,as shown in Fig. 5. The tracking errors cause TSM s_1 and s_2 to approach zero and then converge to $e_1 = 0$, $\dot{e}_1 = 0$, $e_2 = 0$ and $\dot{e}_2 = 0$, respectively, along TSM $s = 0$, in finite time and in the first few seconds of the simulation.

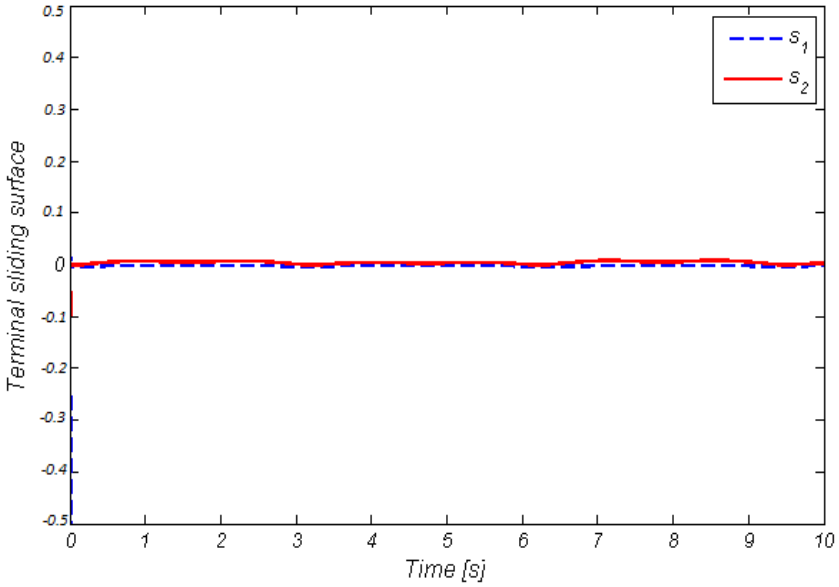

a) master manipulator

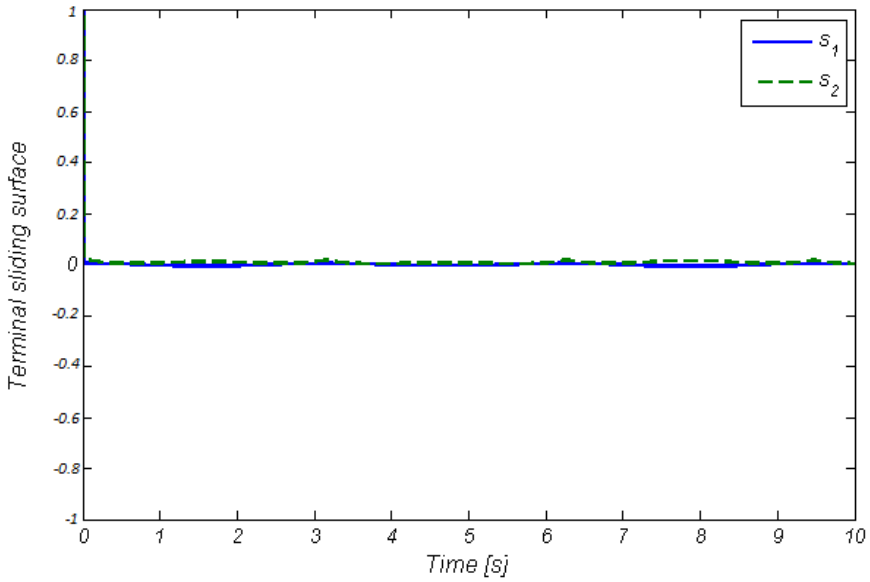

b) slave manipulator

Figure 6: Continuous TSM control of a two-link robot

The precise velocity tracking simulation results of are shown in Figs. 7 and 8. It is clear that the velocity of each slave system link follows the velocity of each master manipulator link, respectively, which tracks the desired reference velocity. The input control torques that are applied to the motors of both joints demonstrate [lead to] continuous and chatter-free τ for the master and slave manipulators (as shown in Fig. 9).

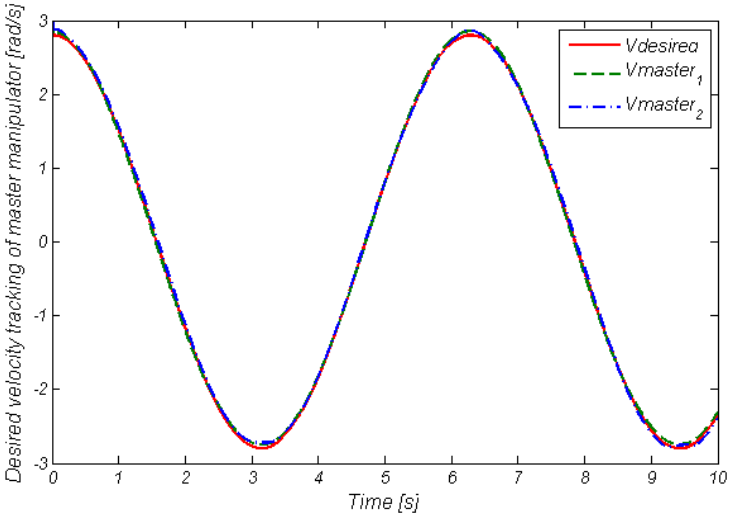

Figure 7: Desired velocity and velocity of master manipulator

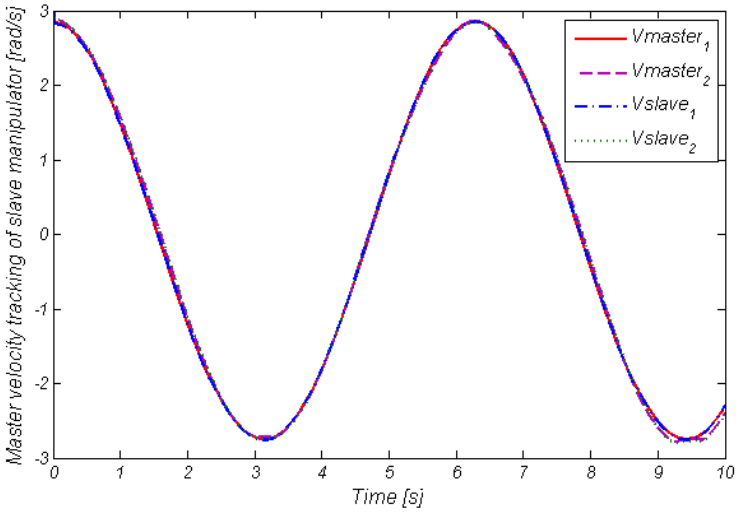

Figure 8: Velocity tracking signals for two-link master and slave manipulators

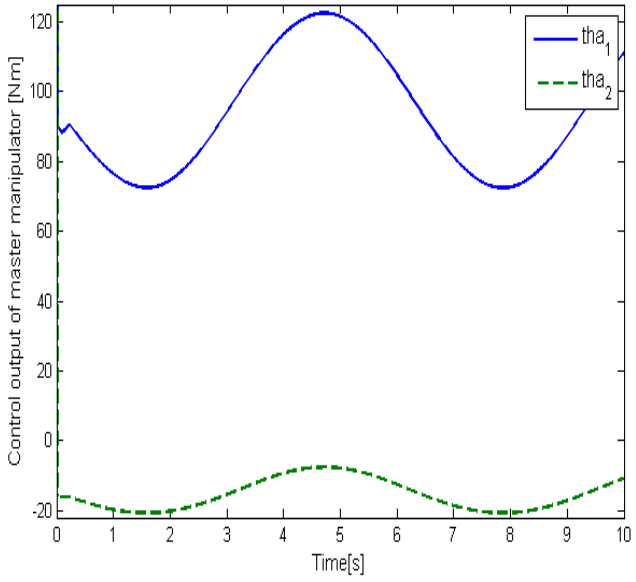

a) τ_{master}

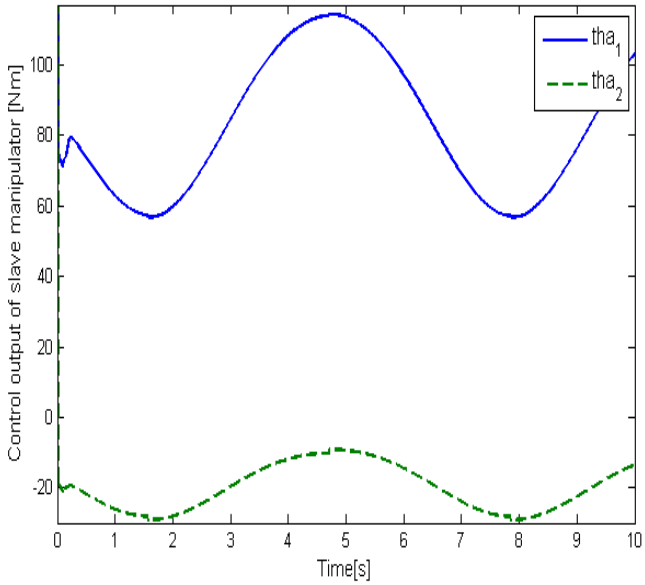

b) τ_{slave}

Figure 9: Controller output

6. Experimental method

The proposed controller is applied for the control of 2-link land based master and slave manipulators with parameter values and features listed in Table 2. The maximum torques are [-0.4, 0.4] Nm and [-0.6, 0.6] Nm for each master and slave joint, respectively, the gear reduction ratio is 1:24, and the encoder resolution of each joint is 1000 pulse/rev. Though, the encoder signals are always subjected to noise, but the practical results are satisfactory. Experimental tests have been performed on the master-slave robots, which are shown in Fig. 10.

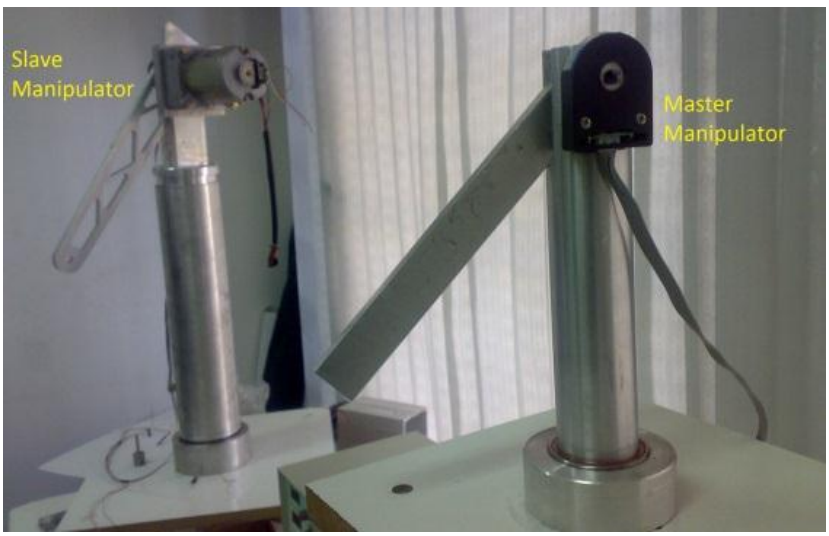

Figure 10: 2-link master-slave manipulators

Table 2: Parameters of links in experimental analysis

Link 1 and 2 parameters	Value
m_1	0.52 m
m_2	0.531 m
l_1	0.45 m
l_2	0.4 m
J_1	0.005
J_2	0.009
C_{d1}	0.1624
C_{d2}	0.078

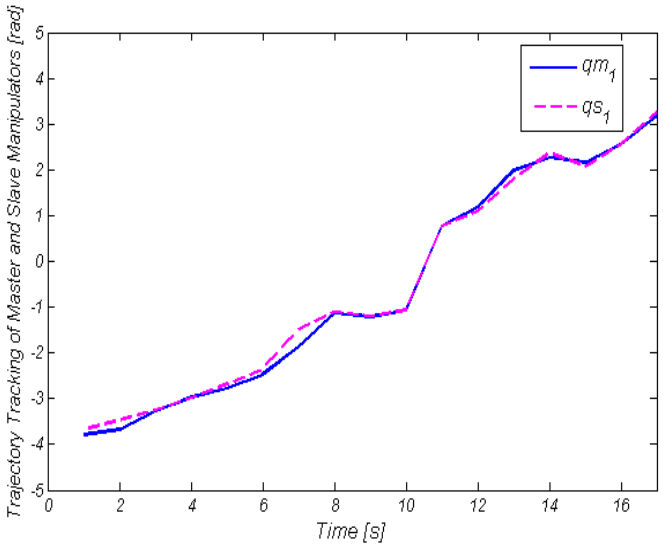

a) Link 1

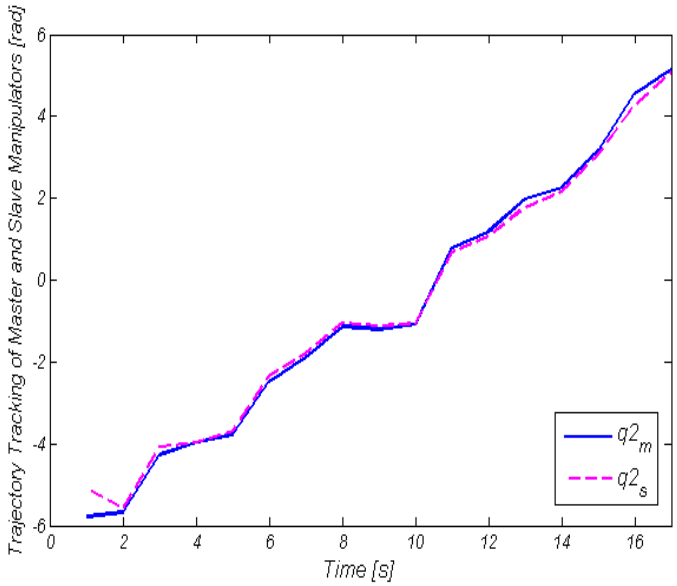

b) Link 2

Figure 11: Position tracking of master manipulator by slave manipulator

Fig. 11 shows the best position tracking performance in land-based master-slave manipulators, which causes the tracking errors and sliding surface (shown in Fig. 12 and Fig. 14) to be very small and the torques (which are applied to the motors of each joint shown in Fig. 13) to be continuous and chatter-free.

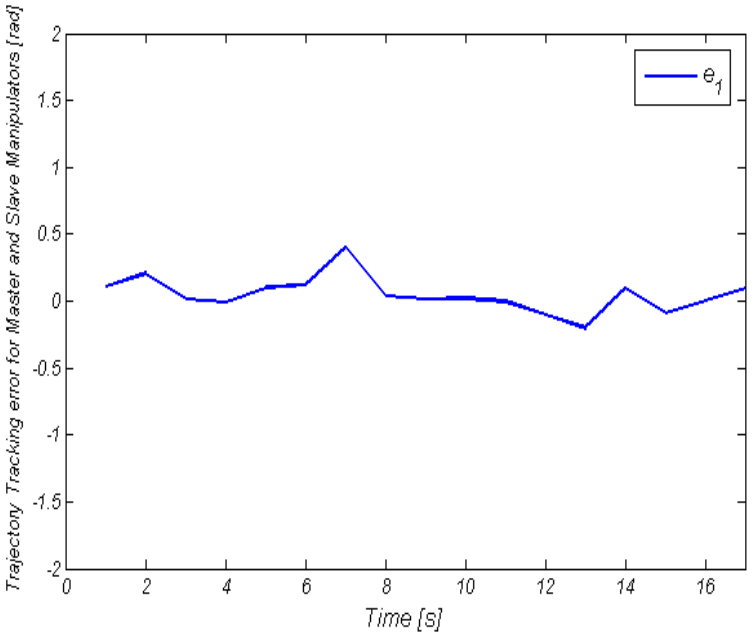

a) link 1

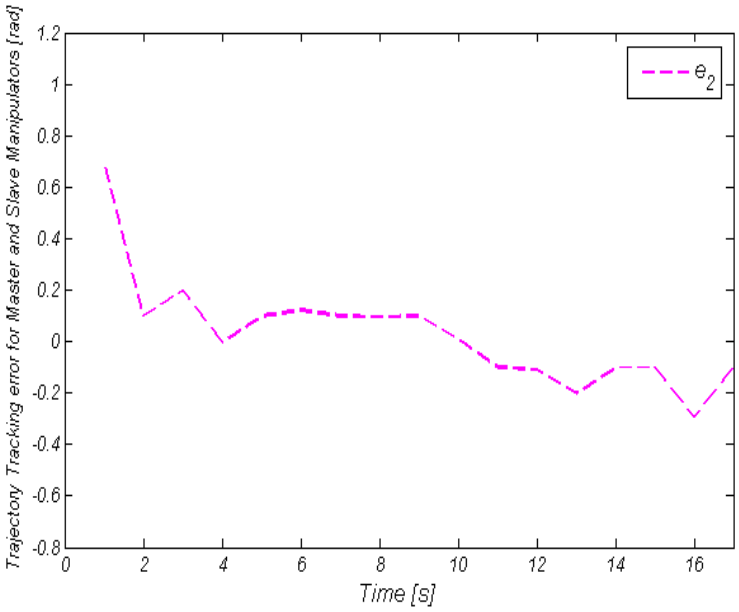

b) Link 2

Figure 12: Tracking error of master-slave manipulators

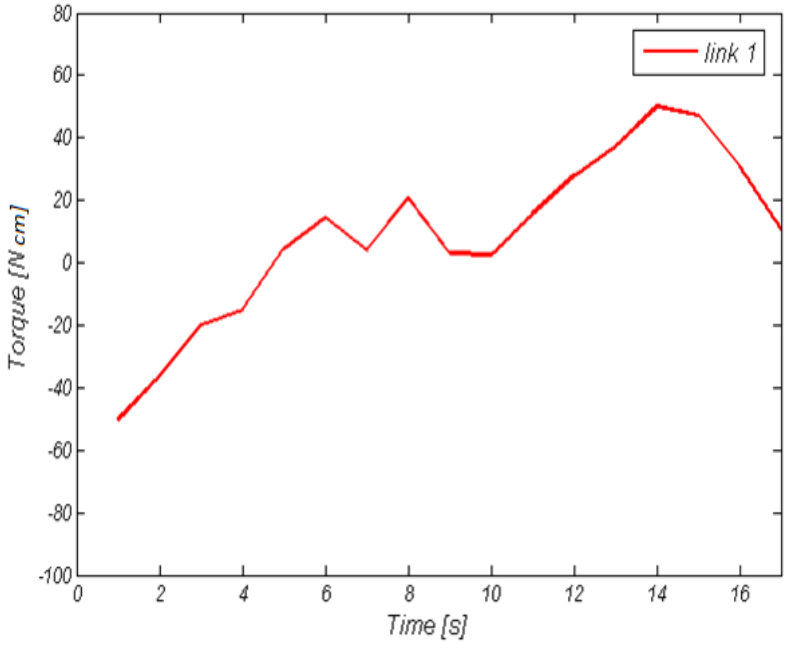

a) Link 1

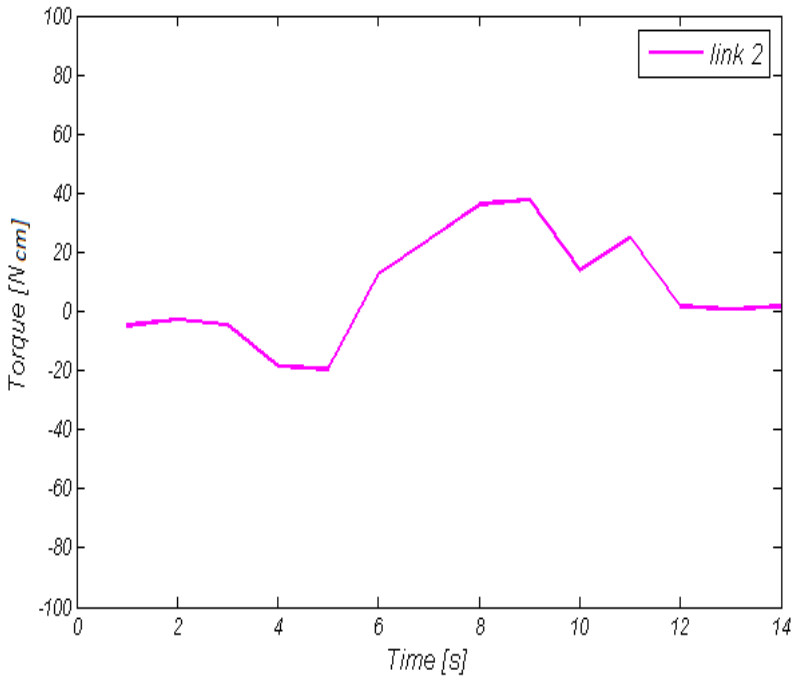

b) Link 2

Figure 13: Control torques of links a) 1 and b) 2

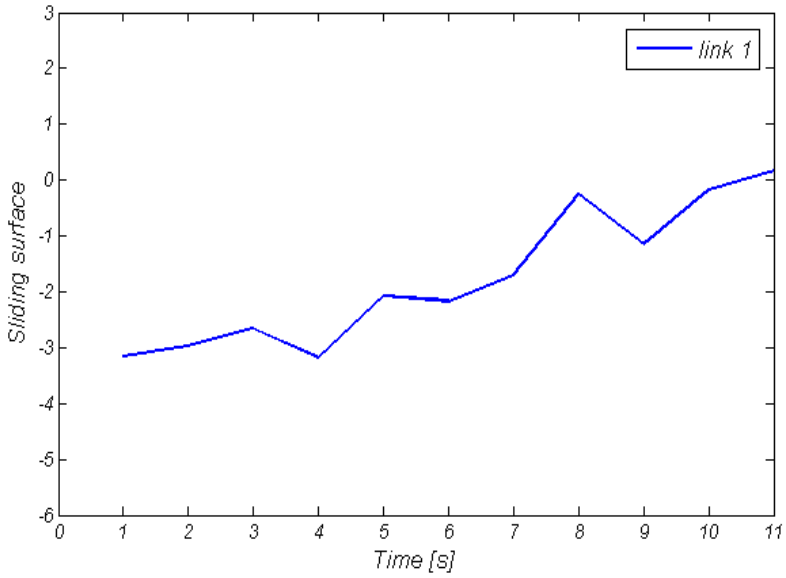

a) Link 1

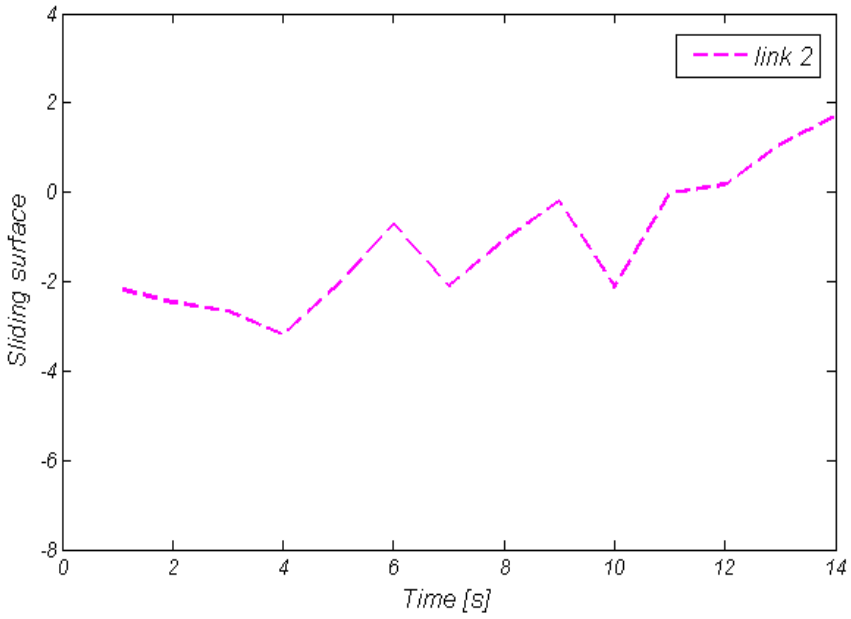

b) Link 2

Figure 14: Terminal sliding surface of links a) 1 and b) 2

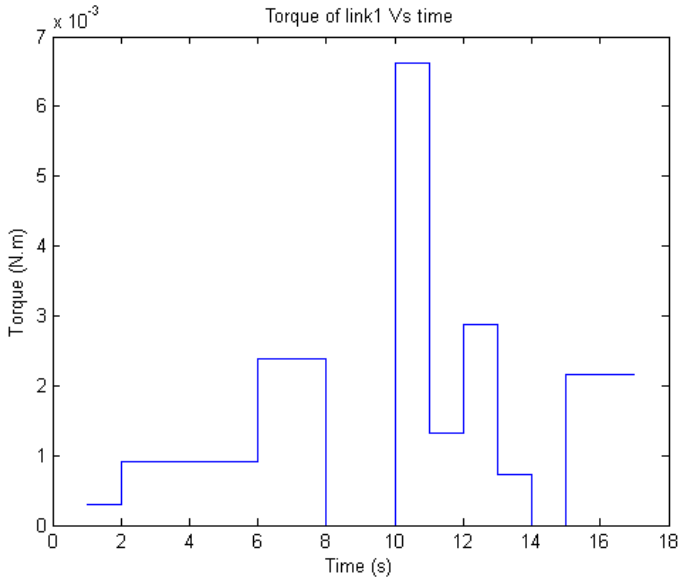

a)

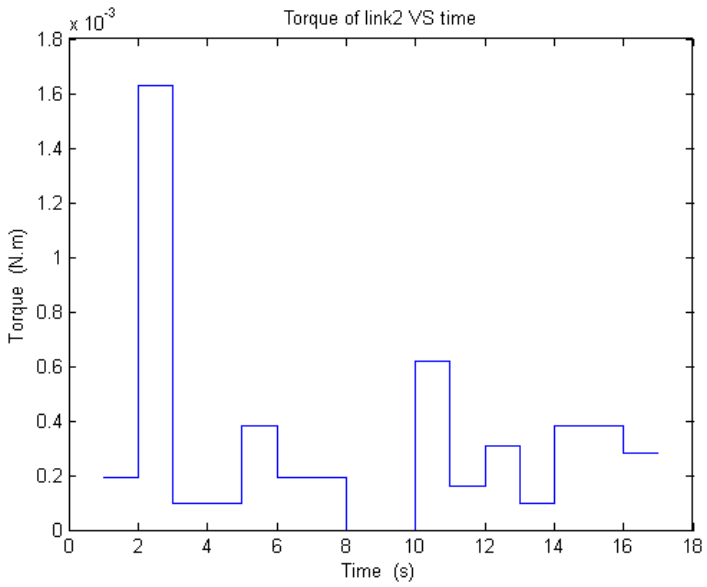

b)

Figure 15: Torques exerted by the air on a) link1 and b) link2

As can be seen the aerodynamic forces and the friction between the air and links are very small, so they are ignored.

In underwater conditions, hydrodynamic forces and torques exerted by water on the links should also be considered. Simulation results show that the drag coefficient for link1 and link2 are 0.1624 and 0.078 respectively and shown in Fig17 in appendix.

By using the drag coefficient and speed of links in different intervals, the torque exerted by the water on link 1 and link 2, are calculated and shown in Fig 16.

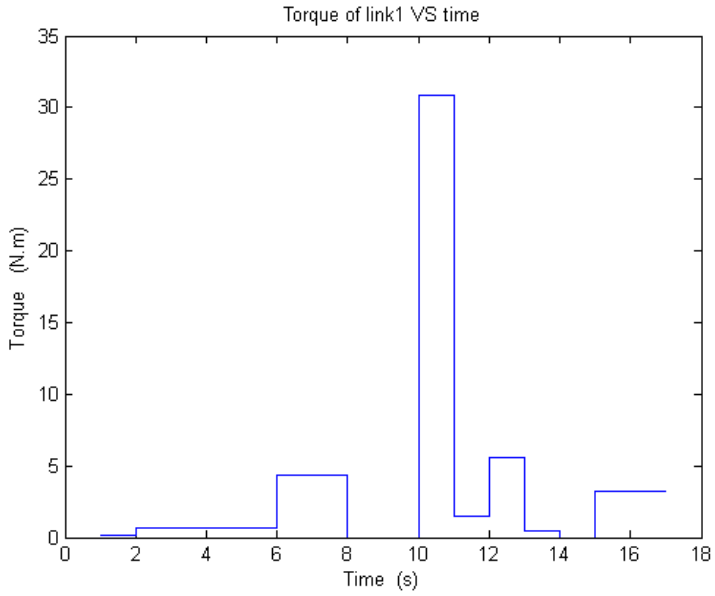

a)

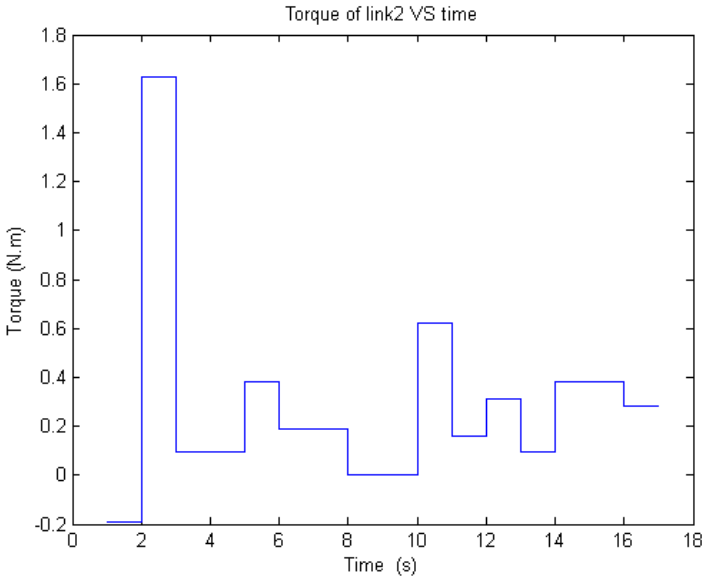

b)

Figure 16: Hydrodynamic torques of (a) link1 and (b) link

Conclusion

A continuous TSM controller with finite-time convergence capability and adaptive control mechanism was presented for the trajectory tracking of master-slave manipulators. The proposed controller has a high precision and it requires no previous knowledge of the bounds of uncertainties and external disturbances, because the adaptive control scheme is proficient in estimating them. In this controller, the chatter reduction capability was augmented by the implementation of a boundary layer method. Then, the problem of synchronizing two different systems was investigated. To make the output of the underwater slave manipulator robustly track the output of the surface master manipulator in finite time, these two systems were considered with different dynamics and totally unknown parameters and external disturbances in the robust adaptive terminal sliding mode control scheme. The applied controller has the advantage of being precise and robust in the presence of uncertainties and hydrodynamic disturbances. The simulation results showed that the slave manipulator accurately tracks the position and velocity of the master manipulator, which precisely

follows the reference position and velocity inputs. The position and velocity tracking errors of the master and slave manipulators were forced to approach zero [and being connivance. The above claims were verified by experimental results. It is emphasized that an improved continuous finite-time robust adaptive terminal sliding mode control scheme with completely considered dynamics has not yet been suggested for synchronizing a land-based master manipulator and an underwater slave manipulator.

References

[1] Dunnigan. M. W., Lane. D. M., Clegg, A.C. and Edwards, "Hybrid position/force control of a hybrid underwater manipulator," lEEE Proc-Control Theory AppL. J. Vol.143, (1996), pp.145-15.

[2] Timothy. W. M, Stephen. M. R, "Development and Experimental Validationof an Underwater Manipulator Hydrodynamic Model," The International Journal of Robotics Research. Vol.17, (1998), pp.748-756.

[3] Kwon. D-Soo, Ryu. J-Hwan, "Design of a Teleoperation Controller for an Underwater Manipulator," International Conference on Robotics & Automation, IEEE, (2000).

[4] Hoang. N.Q, Kreuzer. E, "A Robust Adaptive Sliding Mode Controller for Remotely Operated Vehicles.TechnischeMechanik," (2007)

[5] Sage. H. G, De Mathelin. M. F, Ostertag. E, "Robust control of robot manipulators: A survey," International Journal of Control, Vol. 72, (1999), pp.1498-1522.

[6] Haimo. V. T, "Finite time controllers," Control and Optimization (SIAM), (1986), Vol. 24, pp. 760-770.

[7] Hong. Y, J. Huang, Xu. Y, "an output finite-time stabilization problem," IEEE Transactions on Automatic Control, (2001), Vol. 46, pp. 305-309.

[8] Hong. Y., J. and Huang. Xu. Y, "Finite - time control for robot manipulators," Systems & Control. L, (2002), Vol. 46, pp.243-253.

[9] Slotine. J. J. E, "Applied nonlinear contro," Prentice Hall, Englewood Cliffs, NJ, (1991).

[10] Yu. X., Man. Z., "Fast terminal sliding-mode control design for nonlinear dynamical systems," IEEE Transactions on Circuits and Systems I: Fundamental Theory and Applications, (2002), Vol. 49, pp. 261-264.

[11] Cristi. R, Papoulias. F, Healey, A. J, "Adaptive sliding mode control of autonomous underwater vehicles in the dive plane," IEEE of Oceanic Engineering J, (1990), Vol.15, pp. 152-159.

[12] Walchko. K. J, Novick. D, Nechyba. M. C, "Development of a sliding mode control system with extended Kalman filter estimation for Subjugator. In: Paper submitted to the Florida Conference on recent advances in robotics," (1990), FAU, Dania Beach, FL.

[13] Rahman. I. A, Suboh S. M, "Theory and Design Issues of Underwater Manipulator. International confonCIM," (2007), Malaysia.

[14] Yu. Shuanghe, Yu. Xinghuo, B. Shirinzadeh, Zh. Man, "Continuous finite-time control for robotic manipulators with terminal sliding mode," Automatica Vol. 41, (2005) pp. 1957–1964.

[15] Antonelli. G, "Motion and force control of vehicle-manipulator systems," Int. Springer. J, (2012), Vol. 67, pp. 61-73.

[16] McLain. T. W, Rock. S. M, "Development and Experimental Validation of an Underwater Manipulator Hydrodynamic Model," Robotics Research. J, (1998), Vol. 17, pp. 748-759.

[17] Suboh. S. M. and, Rahman I. A, "Modeling and Control of 2-DOF Underwater Planar Manipulator," (1995) USM Robotics Research Group, Malaysia.

[18] Feng. Y, Yu. X. Man. Z, "Non - singular terminal sliding mode control of rigid manipulators," Automatica. Vol. 38, (2002), pp. 2159–2167.

[19] Jin. M, Lee. J., Chang. P. H, and Choi, Ch, "Practical Nonsingular Terminal Sliding-Mode Control of Robot Manipulators for High-Accuracy Tracking Control," IEEE Transactions on Industrial Electronics. Vol. 56, 9, (2009), pp. 3593-3601.

[20] Pourmahmood. M, Khanmohammadi S, Alizadeh. GH, "Synchronization of two different uncertain chaotic systems with unknown parameters using a robust adaptive sliding mode controller," Commun Nonlinear SciNumer Simulat. Vol. 16, (2011), pp. 2853-2868.

Appendix A

- **Dynamic equation for an underwater slave manipulator**

$$\begin{bmatrix} a_{11}(q_2) & a_{12}(q_2) \\ a_{21}(q_2) & a_{22} \end{bmatrix}\begin{bmatrix} \ddot{q}_1 \\ \ddot{q}_2 \end{bmatrix}+\begin{bmatrix} c_1(q_1,q_2) \\ c_2(q_1,q_2) \end{bmatrix}+\begin{bmatrix} h_1(q_1,q_2)g \\ h_2(q_1,q_2)g \end{bmatrix}+ \begin{bmatrix} F_1^*(dq_1) \\ F_2^*(dq_2) \end{bmatrix}+\begin{bmatrix} D_1(dq_1) \\ D_2(dq_2) \end{bmatrix}=\begin{bmatrix} \tau_1 \\ \tau_2 \end{bmatrix}+\begin{bmatrix} \tau_{d1} \\ \tau_{d2} \end{bmatrix} \quad \text{Eq. (A.1)}$$

where

$$a_{11}(q_2)=m_{a2}l_2^{\,2}+2l_1l_2m_{a2}\cos(q_2)+(m_{a1}+m_{a2})l_1^{\,2} \quad \text{Eq. (A.2)}$$

$$a_{12}(q_2)=m_{a2}l_2^{\,2}+l_1l_2m_{a2}\cos(q_2) \quad \text{Eq. (A.3)}$$

$$a_{21}(q_2)=m_{a2}l_2^{\,2}+l_1l_2m_{a2}\cos(q_2) \quad \text{Eq. (A.4)}$$

$$a_{22}=m_{a2}l_2^{\,2} \quad \text{Eq. (A.5)}$$

$$c_1(q_1,q_2)=-l_1l_2m_{a2}\sin(q_2)dq_2dq_1- l_1l_2m_{a2}\sin(q_2)(dq_1+dq_2)dq_2 \quad \text{Eq. (A.6)}$$

$$c_2(q_1,q_2)=l_1l_2m_{a2}\sin(q_2)dq_1dq_1 \quad \text{Eq. (A.7)}$$

$$h_1(q_1,q_2)g=(m_2-\nabla_2)l_2g\cos(q_1+q_2)+ (m_1+m_2-\nabla_1-\nabla_2)l_1g\cos(q_1) \quad \text{Eq. (A.8)}$$

$$h_2(q_1,q_2)g=(m_2-\nabla_2)l_2g\cos(q_1+q_2) \quad \text{Eq. (A.9)}$$

$$F_1^*(dq_1)=k_{c1}\,\mathrm{si}\,g\,\mathrm{n}(dq_1)+k_{v1}dq_1 \quad \text{Eq. (A.10)}$$

$$F_1^*(dq_1)=k_{c2}\,\mathrm{si}\,g\,\mathrm{n}(dq_2)+k_{v2}dq_2 \quad \text{Eq. (A.11)}$$

$$D_1(dq_1)=0.5\rho c_d\,l_1dq_1^{\,2} \quad \text{Eq. (A.12)}$$

$$D_2(dq_2)=0.5\rho c_d\,l_2dq_2^{\,2} \quad \text{Eq. (A.13)}$$

- **Dynamic equation for a master manipulator**

Meanwhile dynamic equation for a two link land based master system is obtained as

$$\begin{bmatrix} a_{11}(q_2) & a_{12}(q_2) \\ a_{21}(q_2) & a_{22} \end{bmatrix}\begin{bmatrix} \ddot{q}_1 \\ \ddot{q}_2 \end{bmatrix}+\begin{bmatrix} c_1(q_1,q_2) \\ c_2(q_1,q_2) \end{bmatrix}+\begin{bmatrix} G_1(q_1,q_2)g \\ G_2(q_1,q_2)g \end{bmatrix}= \begin{bmatrix} \tau_1 \\ \tau_2 \end{bmatrix}+\begin{bmatrix} \tau_{d1} \\ \tau_{d2} \end{bmatrix} \quad \text{Eq. (A.14)}$$

$$a_{11}(q_2)=m_1\left(\frac{l_1}{2}\right)^2+m_2\left(\frac{l_2}{2}\right)^2+ m_2l_1^{\,2}+l_1l_2m_2\cos(q_2) \quad \text{Eq. (A.15)}$$

$$a_{12}(q_2)=m_2\left(\frac{l_2}{2}\right)^2+\left(\frac{l_1l_2}{2}\right)m_2\cos(q_2) \quad \text{Eq. (A.16)}$$

$$a_{21}(q_2)=m_2\left(\frac{l_2}{2}\right)^2+\left(\frac{l_1l_2}{2}\right)m_2\cos(q_2) \quad \text{Eq. (A.17)}$$

$$a_{22}=m_2\left(\frac{l_2}{2}\right)^2 \quad \text{Eq. (A.18)}$$

$$c_1(q_1,q_2) = -l_1 l_2 m_2 \sin(q_2) dq_2 dq_1 - \left(\frac{l_1 l_2}{2}\right) m_2 \sin(q_2)(dq_1 + dq_2) dq_2 \quad \text{Eq. (A.19)}$$

$$c_2(q_1,q_2) = \left(\frac{l_1 l_2}{2}\right) m_2 \sin(q_2) dq_1 dq_1 \quad \text{Eq. (A.20)}$$

$$G_1(q_1,q_2)g = m_2\left(\frac{l_2}{2}\right) g\cos(q_1+q_2) + (m_1+2m_2)\left(\frac{l_1}{2}\right) g\cos(q_1) \quad \text{Eq. (A.21)}$$

$$G_2(q_1,q_2)g = m_2\left(\frac{l_2}{2}\right) g\cos(q_1+q_2) \quad \text{Eq. (A.22)}$$

Appendix B

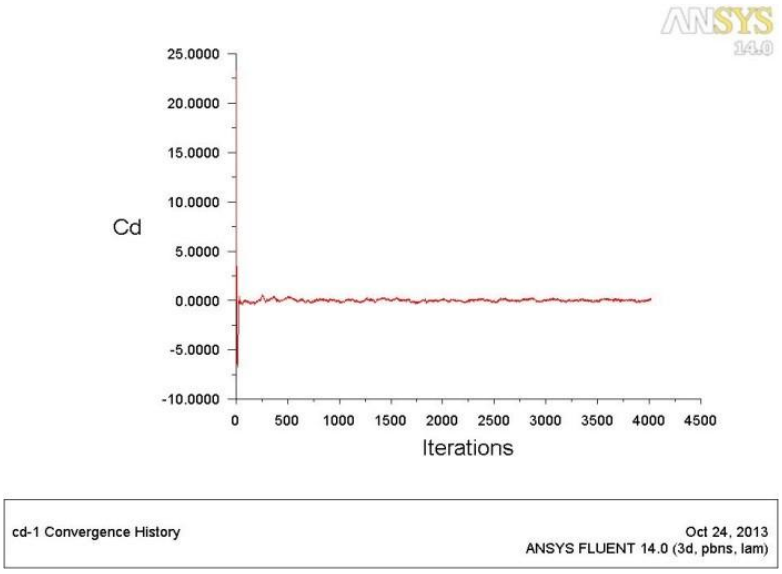

a)

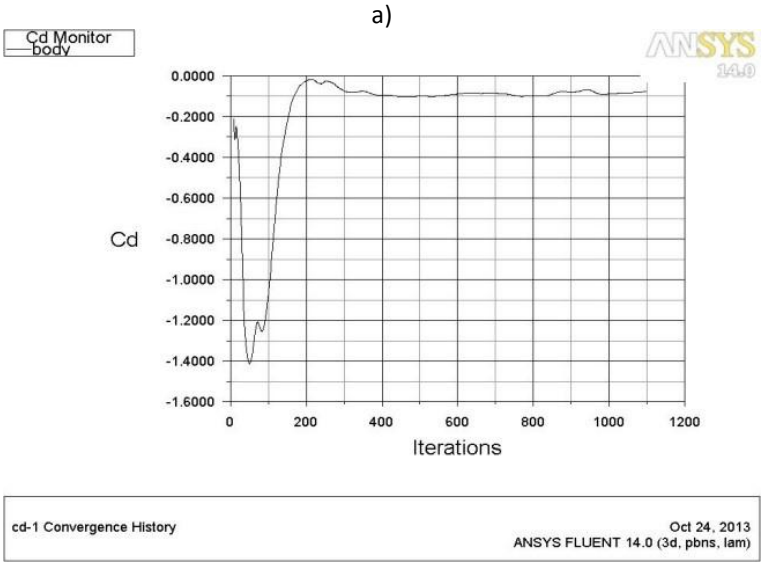

b)

Figure B.1: Drag coefficient of (a) link 1 (b) link 2

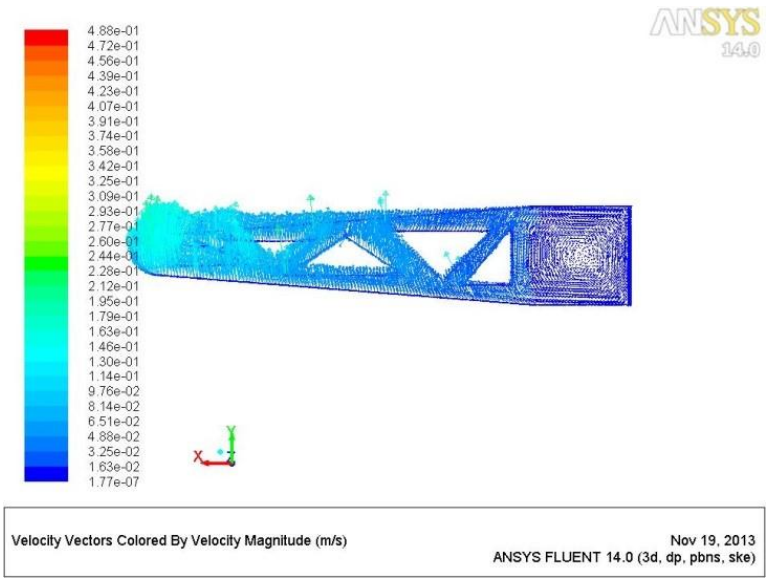

a)

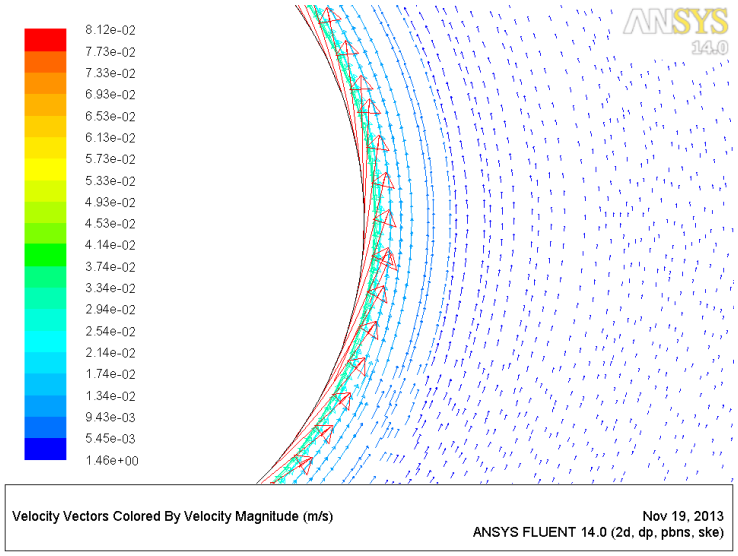

b)

Figure B.2: Velocity contour of (a) link 1 and (b) link2